Stabilizing Control of Series Capacitor Power System Using a Superconducting Magnetic Energy Storage Unit under unequal α-mode

www.serd.ait.ac.th/reric

A. Abu-Siada, S. Islam, and W. B. Lawrance
Department of Electrical Engineering
Curtin University of Technology, Bentley, WA6102
AUSTRALIA

ABSTRACT

This paper investigates the use of Superconducting Magnetic Energy Storage (SMES) unit to stabilize multi-mode torsional oscillations of Sub-Synchronous Resonance (SSR) oscillations of a turbine-generator set at the same time to improve dynamic transient stability of the studied system under different operating conditions. Two-control algorithm are discussed, they are equal α-mode and unequal α-mode of the converter stations of the SMES unit. Results show that the designed controller provides proper damping to all oscillating modes a swing mode simultaneously. Eigenvalues analysis is used to show the effectiveness of the proposed controller in stabilizing all modes of oscillations of the system under different operating conditions. The proposed controller is simple and easy to be implemented.

1. INTRODUCTION

It is well known that series-capacitor compensation benefits power system in several ways such as improving transient stability, enlarging power transfer capability, etc. However, SSR problems usually occur in a steam turbine-generator connected to a series-capacitor compensated lines [1]. When the degree of series capacitor compensation is increased, an electric resonance of the generator, transformer, transmission lines, and series capacitor may develop, usually at subsynchronous frequency. If the resonant frequency becomes complementary with that of the torsional oscillation of the mass spring of the mechanical system, they will be mutually excited, causing serious shaft failures and other damages. The first two shaft failures caused by SSR occurred at Mohave station in 1970 and 1971, respectively[2]. Since then, an extensive contribution has been made to increase torsional mode damping and many countermeasures have been suggested to increase torsional mode damping such as block filter[3], excitation control[4], static VAR compensator[5], HVDC[6], static phase shifter[7], by pass filter[8], Power System Stabilizers (PSS)[9], optimal control of the turbine governor system and the use of shunt reactor[10-12]. The natural frequencies of torsional oscillations range normally 15-45 Hz, whereas the inertia frequency of oscillation of the coupled electromechanical system, that is dynamic transient oscillation, is about 1-2 Hz. Thus the conventional lead-lag type PSS, which are designed on the basis of classical control theory, cannot guarantee all oscillation modes[10].

Due to the rapid development of high temperature superconducting materials, applications of the superconductor in power systems have received much attention. Since the first 30-MJ SMES unit was successfully commissioned at Bonnevile Power Administration (BPA) substation in Tacoma, Washington, in February 1983, investigation of SMES on power systems has been quickly and extensively developed[13, 14]. One of the most basic properties of the superconducting materials is the ability to give up electrical resistivity. Therefore, superconductors carry electricity without any energy losses, as most conductors do. The SMES system was developed to take advantage of this property. Since the coil is lossless, the energy can be released almost instantaneously with a very high efficiency. It was estimated that a unit could be over 90% efficient (including refrigeration losses)[15]. With an appropriate mechanism, this energy can be injected into an electrical system to boost voltage when needed. Although the original purpose of the SMES unit is using it as a load leveling and load management[16], the unit can also be applied to be a transmission line stabilizer and load frequency controller[17], or to damp out low frequency electromechanical oscillations and increase the stability of power system[18]. SMES can be viewed as a Flexible AC Transmission System (FACTS), with the added dimension that can insert/absorb real power into/from the grid. For each application, different system specifications and different control algorithms are needed[19-21].

In this paper, a SMES controller with unequal α-mode to control the firing angles of the SMES converters is proposed in order to damp effectively all SSR oscillation modes. The controller gains are selected based on modal control theory. In addition, a frequency-domain approach based on eigenvalue analysis and a time domain approach based on dynamic response simulations will also be utilised to obtain a detailed simulation outcome.

2. SMES PLANT DESCRIPTION

Fig. 1 shows the main components of the SMES unit. It consists of a high temperature superconductors (HTS) coil that must be maintained within the superconductivity state by means of a cryogenic medium (e.g. liquid helium or nitrogen). The superconductor coil is interfaced with a power system through a pair of bi-directional AC/DC converters connected at the low-tension sides of two separate Y-Y, Y-Δ transformers.

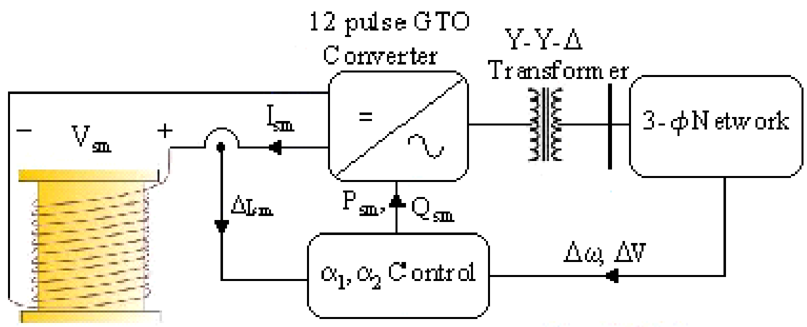

Fig. 1 Schematic single line diagram of the SMES unit

Consequently the AC voltages applied to each six pulse valve group that make up the twelve pulse valve group have a phase difference of 30 degrees which is utilized to cancel the AC side 5th and 7th harmonic currents and DC side 6th harmonic voltage, thus resulting in a significant saving in harmonic filters[22]. The current I_{SM} passing through the superconducting inductor is unidirectional; however, the voltage V_{SM} across the inductor terminals can be varied in a wide range between positive and negative values through the control of firing angles α_1 and α_2. In this way both active and reactive power of the power system can be modulated.

3. DESCRIPTION OF THE STUDIED SYSTEM

Fig. 2 shows the system under study, which consists of a turbine-generator connected to a large power system via step-up transformer and a series-capacitor compensated transmission line.

Also, a local AC load is connected to the generator bus bar. The turbine-generator mechanical system is modelled as a linear four-mass spring dashpot system. These masses are high-pressure turbine (HP), Low-pressure turbine (LP), generator (GEN) and exciter (EX). In such a model, each major rotating element is modelled as a lumped mass and each shaft segment is modelled as a mass-less rotational spring with its stiffness given by the spring constant. Viscous damping of each mass is represented in the model. The suggested location of the SMES unit is at the terminals of the synchronous machine to provide adequate damping for the turbine generator set.

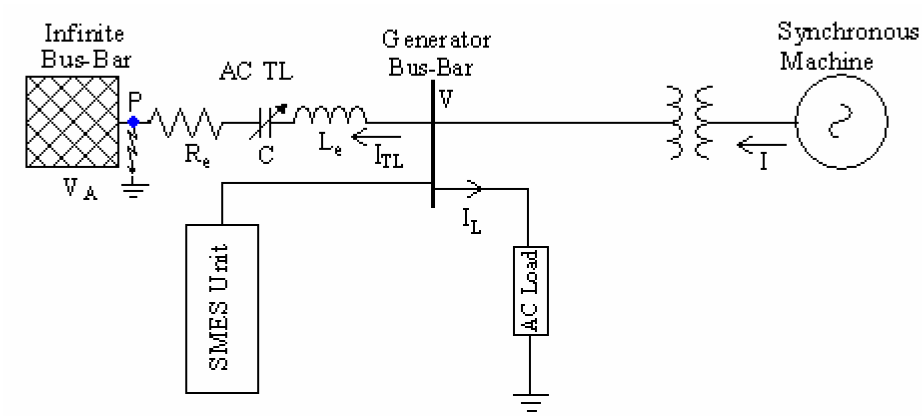

Fig.2 Single line diagram of the system under study

4. THE P-Q SIMULTANEOUS CONTROL SCHEME OF SMES UNIT

In accordance with converter theory, the voltage V_{sm} in the DC side of the bridge is expressed by[23]:

$$V_{sm} = V_{smo}(\cos\alpha_1 + \cos\alpha_2) \tag{1}$$

where, V_{smo} = the ideal no-load maximum DC voltage of the 6-pulse bridges.

The current and voltage of the superconducting inductor are related by:

$$I_{sm} = \frac{1}{L_{sm}}\int_{t_o}^{t} V_{sm}\,d\tau + I_{smo} \tag{2}$$

where, I_{smo} = the initial current of the inductor.

For "charging" at the maximum rate, clearly V_{sm} should be held at its maximum positive rate. The inductor current I_{sm} raises exponentially and magnetic energy W_{sm} is stored in the inductor. When the inductor current reaches its rated value I_{smo}, it is maintained constant by lowering the voltage across the inductor to zero. At any time during the charging period, the amount of energy stored in the magnetic field is expressed by:

$$W_{sm} = \int \frac{B^2}{2\mu_o}\,dV \tag{3}$$

$$= \frac{1}{2} L_{sm} I_{sm}{}^2 \tag{4}$$

where B is the magnetic field, V is the volume of the coil, and μ_o is a constant that represents magnetic permeability of the material through which the magnetic field must pass. Eq. 3 shows that the stored energy is related to the strength of the magnetic field in the coil. However Eq. 4 shows that the stored energy depends on the current in, and the inductance of the coil. The current I_{sm} is an integral function of V_{sm} as given by Eq. (2). It can never reverse its direction, so it can only have positive values. At any time, the active and reactive power delivered or absorbed by the SMES unit is given by:

$$P_{sm} = V_{smo} I_{sm} (cos\,\alpha_1 + cos\,\alpha_2) \tag{5}$$

$$Q_{sm} = V_{smo} I_{sm} (sin\,\alpha_1 + sin\,\alpha_2) \tag{6}$$

Because V_{sm} is uniquely defined by α_1 and α_2, its value can be varied in a wide range of positive and negative values via the control of α_1 and α_2. I_{sm} is always unidirectional. Thus reversibility as well as magnitude control of power flow is achieved continuously and smoothly through the control of both firing angles α_1 and α_2 as can be concluded from Eqs. (5) and (6). Using Eqs. (5) and (6), the firing angles of the converter under four-quadrant operation can be calculated as[18]:

$$\alpha_1 = cos^{-1}\left(\frac{P_{sm}}{\sqrt{P_{sm}^2 + Q_{sm}^2}}\right) + cos^{-1}\left(\frac{\sqrt{P_{sm}^2 + Q_{sm}^2}}{2V_{smo} I_{sm}}\right) \tag{7}$$

$$\alpha_2 = cos^{-1}\left(\frac{P_{sm}}{\sqrt{P_{sm}^2 + Q_{sm}^2}}\right) - cos^{-1}\left(\frac{\sqrt{P_{sm}^2 + Q_{sm}^2}}{2V_{smo} I_{sm}}\right) \tag{8}$$

In order to use the SMES unit as a torsional mode stabilizer, the active power P_{sm} transferred in the converter is controlled continuously depending on the measured speed deviation of the turbine-generator rotor. The reactive power control is usually for the purpose of voltage stabilization. Then the reactive power Q_{sm} transferred in the converter is controlled continuously depending on the measured voltage deviation of the generator bus terminal. Fig. 3 shows the proposed SMES controller for simultaneous control of P-Q modulation of the SMES unit.

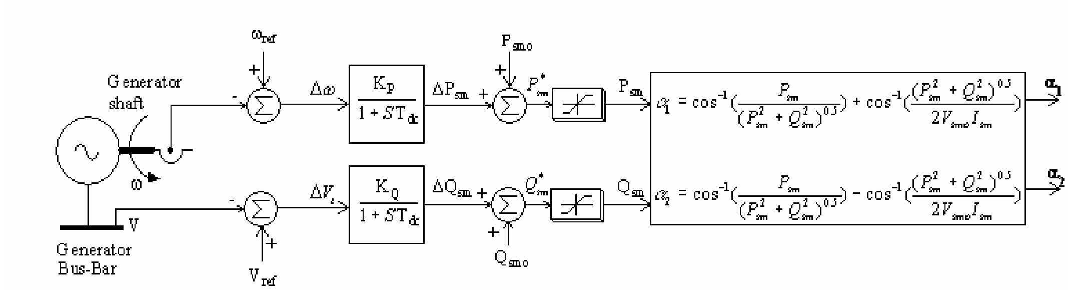

Fig. 3 Proposed SMES Controller

In Fig. 3, the generator shaft speed deviation ($\Delta\omega$) is fed to generate the active power deviation (ΔP_{sm}) while the generator terminal voltage deviation (ΔV_t) is sensed to generate the reactive power deviation (ΔQ_{sm}). Both deviations are respectively added to the nominal active power (P_{smo})

and reactive power (Q_{smo}) to determine the desired active and reactive power modulation required by the SMES unit. Hardware implementation means the required power modulation must be limited to upper and lower limits; these values of P_{sm} and Q_{sm} are used to determine the desired firing angles α_1 and α_2 in order that the output active and reactive power of the SMES unit can be decided. In Fig. 3, K_P and K_Q are the control loop gains while T_{dc} is the transducer time constant.

If $\alpha_1 = \alpha_2$ is chosen, the value of active and reactive power consumed by the SMES unit (P_{sm} and Q_{sm}) may or may not be equal to desired active and reactive power modulation (P^*_{sm} and Q^*_{sm}). The firing angles under equal-α mode are calculated as:

$$\alpha_1^* = \alpha_2^* = \alpha = tan^{-1}(Q^*_{sm} / P^*_{sm}) \tag{9}$$

For a particular value of inductor current, the locus of P-Q modulation is a circle of radius $2V_{smo}I_{sm}$. The commutating reactance has been neglected. If the variation of the inductor current is small, for large value SMES inductance, then one can write

$$2\,V_{smo}I_{sm} = 2\,V_{smo}I_{smo} = S_{max} \tag{10}$$

where, S_{max} = the maximum MVA available in the SMES unit.

Therefore, $P_{sm} = S_{max}\,cos\alpha$ and $Q_{sm} = S_{max}\,sin\alpha$ and the possible power operating range for SMES unit can be depicted in Fig. 4. It is bounded by two circles, having radial length of S_{min} and S_{max} respectively.

The value of active and reactive power consumed by the SMES unit (P_{sm} and Q_{sm}) may or may not be equal to the desired active and reactive power modulation (P^*_{sm} and Q^*_{sm}), which can be viewed in Fig. 4 [24].

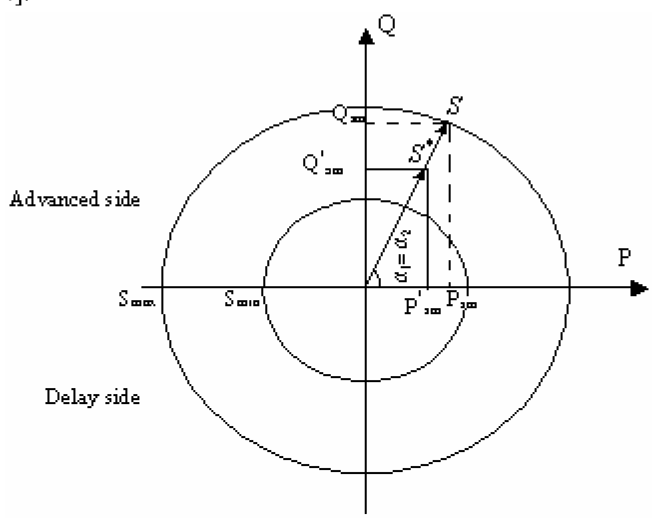

Fig. 4 P-Q circular diagram under equal α-mode

Defining $S^* = \sqrt{P^{*2}_{sm} + Q^{*2}_{sm}}$,

If $S^* < S_{max}$, then $P^*_{sm} < P_{sm}$ and $Q^*_{sm} < Q_{sm}$

If $S^* > S_{max}$, then $P^*_{sm} > P_{sm}$ and $Q^*_{sm} > Q_{sm}$

It means that the active and reactive power consumption may not help in power system stabilization. It was demonstrated in other studies that there is no improvement in the power system unless an extra controller is added[5, 25]. Under unequal-α mode, the P-Q circular diagram is modified to be as shown in Fig. 5.

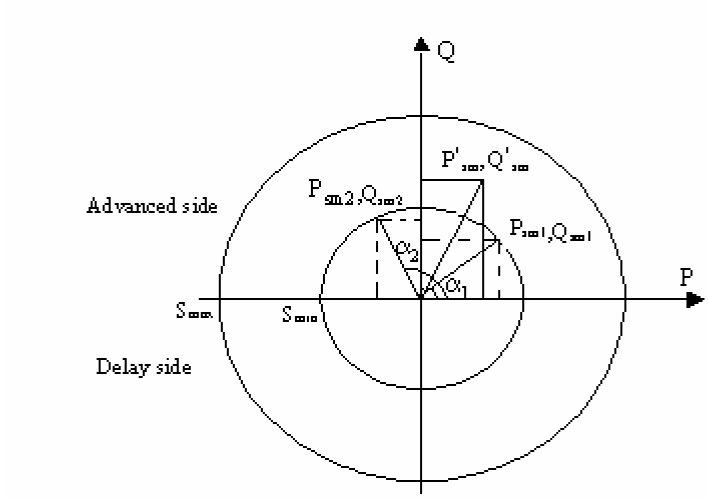

Fig. 5 P-Q circular diagram under unequal α-mode

Unlike the equal α-mode, if $S^* < S_{max}$, then $P_{sm} = P^*_{sm}$ and $Q_{sm} = Q^*_{sm}$. If $S^* > S_{max}$, then $P_{sm} = P^*_{sm}$, and the magnitude of Q_{sm} can be calculated as $Q_{sm} = \sqrt{S^2 - P^{*2}_{sm}}$ and always less than Q^*_{sm} .

5. EIGENVALUE ANALYSIS

Combining the mass-spring system on the generator shaft, armature and field windings, excitation system, governor system, and the capacitor compensated transmission line, a set of 23 order nonlinear differential equations for the system without the SMES unit can be obtained. They can be written in the form:

$$\dot{X} = f\,[\,X, u\,] \tag{11}$$

where,

$$X = [X_1 X_2 X_3 X_4 X_5]', \tag{12}$$

$X_1 = [\omega_g, \delta, \omega_H, \theta_H, \omega_L, \theta_L, \omega_{ex}, \theta_{ex}]$,

$X_2 = [i_a, i_b, i_c, i_{fd}, i_{kd}, i_{kq}]$,

$X_3 = [i_{tl1}, i_{tl2}, i_{tl3}]$,

$X_4 = [P_e, E_{fd}, V_f, E_{c1}, E_{c2}, E_{c3}]$, and

$X_5 = [P_{SM}, Q_{SM}, I_{SM}, \alpha_1, \alpha_2]$.

The control vector u is a supplementary control signal from the PID SMES controller. Under unequal α-mode of operation, there will be no need for using the supplementary control signal. The firing angles α_1 and α_2 are enough to be used as control signals as will be shown in the next section. For small perturbations of the states, the system of Eq. (11) can be linearised around the steady state equilibrium point and can be expressed as:

$$\Delta\dot{X}(t) = A\Delta X(t) + BU(t) \quad (13)$$

where, ΔX is the change of the state vector. The dynamics matrix A in the above equation depends on the parameters and operating conditions of the system under study. B is a constant input matrix. The output equation is:

$$Y(t) = CX(t) = \Delta\omega \quad (14)$$

6. DETERMINATION OF THE SMES CONTROL LOOP GAINS (K_P AND K_Q)

Fig. 6 shows the electromechanical eigenvalue mode for various values of K_P and K_Q where the SMES was located at the generator terminal. The conjugate pair is omitted in Fig. 6.

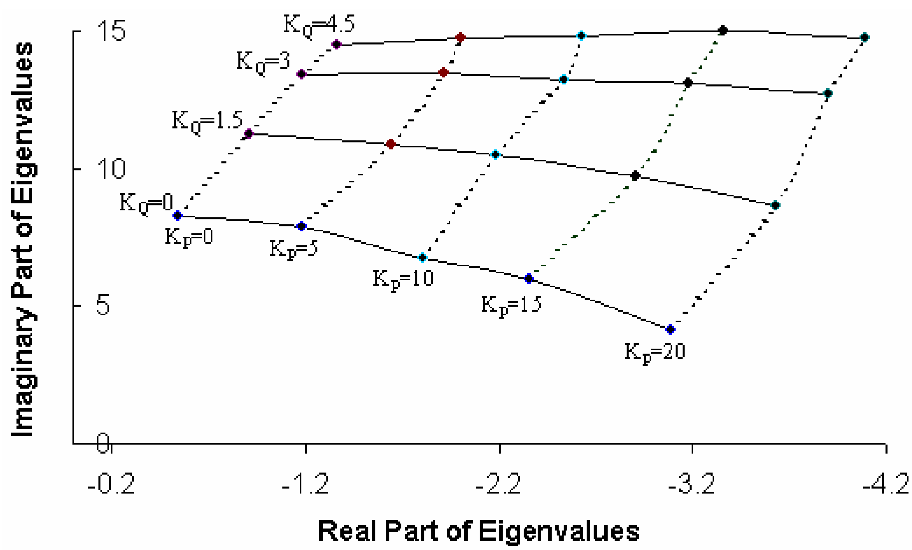

Fig. 6 Root locus of electromechanical mode versus parameters of SMES controller (K_P and K_Q)

In Fig. 6, the effectiveness of the simultaneous control of active and reactive power can be compared with the reactive power control corresponding to K_P= 0 (e.g., SVC) and with the active power control corresponding to K_Q= 0. When the control by SVC is applied (K_P=0), the eigenvalue is shifted to the upper direction in the complex plane, which means that the synchronizing torque T_S is reinforced as the gain K_Q becomes larger while the improvement of damping is small. When the active power control is applied (K_Q= 0), the eigenvalue is shifted to the left, which means that the damping torque T_D is improved as the gain K_P becomes large. On the other hand, the synchronizing torque becomes small. Comparing these two situations together, the synchronizing torque as well as damping can be reinforced at the same time by choosing K_P and K_Q properly when the active and reactive control is applied. Therefore, there is a definite advantage of implementing the simultaneous control of active and reactive power. For the studied system, K_P and K_Q are chosen to be 8.25 and 1.45 respectively.

7. DAMPING OF TURBOGENERATOR SUB-SYNCHRONOUS OSCILLATION

The A matrix in Eq. (13) depends on the degree of series capacitor compensation of the AC transmission line. The compensation factor, given as X_C / X_L, is normally expressed in percent. Table 6.3 shows the eigenvalues of the system for X_C / X_L=0.55, P_0=1 pu, V_t= 1 pu and unity power factor. The eigenvalues of the open-loop system including no SMES are listed in the first column. The eigenvalues of the closed-loop system including the SMES but under equal-α mode of operation are listed in the second column. The eigenvalues of the closed- loop system including the SMES under unequal-α mode of operation are listed in the third column. By investigating the eigenvalues listed in table 6.3 they are shared to three groups as follows:

- the modes which have low frequency and well damping (the modes corresponding to the excitation system),
- the modes which have high frequency and poor damping (the modes corresponding to low and high LC resonance slip frequencies, and torsional oscillations),
- the modes in the neighbourhood of the origin (remaining modes, which include a swing mode, except the modes stated above).

It can be seen from table 1 that the open loop system is unstable as there are two torsional modes located in the right side of s-plane (0.1834 ±j10.9713 and 0.040 ±j10.8809). There is nearly no damping on the low frequency oscillation, which is dominantly affected by the electromechanical mode. Incorporating the SMES unit under equal-α mode of operation to the generator bus will shift these eigenvalues to the left side of s-plane (-0.0511 ±j10.9761 and -0.0554 ±j10.9821). It means the system will be stable however; the damping of oscillating modes is not sufficient. Incorporating the SMES unit under unequal-α mode of operation to the generator bus will shift the unstable modes to significant safe negative values of s-plane (-0.8310 ±j10.9761 and -0.4154 ±j10.9821). The overall performance is improved with the SMES unit under unequal-α mode and the damping effect of the SMES unit to all modes is highly appreciated.

Table 2 shows the eigenvalues of the system under study under the same operating conditions as in table 1 but with P_0 = 1.5 p.u. The eigenvalues of the open-loop system including no SMES are listed in the first column. The eigenvalues of the closed-loop system including the SMES but under equal-α mode of operation are listed in the second column. The eigenvalues of the closed- loop system including the SMES under unequal-α mode of operation are listed in the third column. It can be seen that the open loop system without SMES unit is unstable. By adding the SMES under equal-α mode, there is little improvement in the damping of the oscillatory modes. However, the system is still unstable. If SMES under unequal-α mode of operation is used, there is a great improvement in the damping of all oscillatory modes and all eigenvalues are shifted to the left side of the s-plane.

Fig. 7 plots the real part of the torsional mode 1 under different degrees of series compensation (X_C / X_L) for the same three control schemes. P_0 is fixed at 1 p.u. during this study. It can be seen that, without SMES unit mode 1 is stable up to 50% compensation degree. With SMES unit under equal-α mode of operation the stability margin has been extended to 55% compensation degree. However, with SMES unit under unequal-α mode of operation the torsional mode 1 is always stable at any compensation degree.

It is valuable to note that using SMES unit under unequal-α mode of operation will enhance all the torsional modes of the turbogenerator. Damping of the electromechanical mode is simultaneously greatly improved. The most widely used power system stabilizer (PSS) is not needed to damp the low frequency oscillation since the SMES under unequal-α mode can provide enough damping torque. It can be concluded that the proposed controller gives the required damping characteristics for the system and it can render all SSR modes insensitive to different operating conditions.

Table 1 System eigenvalues at P_0=1.0 p.u., V_t=1 p.u. (X_C/X_L=0.55)

Open-loop system (Without SMES)	Closed-loop system with SMES (equal-α mode)	Closed-loop system with SMES (unequal-α mode)
-0.0987 ±j23.2533	-0.2131 ±j23.3397	-0.2131 ±j23.3397
-0.1412 ±j14.8755	-0.5410 ±j14.4806	-3.5080 ±j14.4806
-0.1026 ±j11.6040	-0.5272 ±j14.3207	-0.7272 ±j14.3207
-0.0286 ±j11.0482	-0.0591 ±j13.3773	-0.4391 ±j13.3773
-0.1212 ±j11.0195	-0.1470 ±j13.3735	-0.4050 ±j13.3735
0.1834 ±j10.9713	**-0.0511 ±j10.9761**	**-0.8310 ±j10.9761**
-0.1381 ±j10.9243	-0.1584 ±j10.9753	-0.3321 ±j10.9753
0.040 ±j10.8809	**-0.0554 ±j10.9821**	**-0.4154 ±j10.9821**
-0.0043± j1.9717	-0.0564 ±j13.3649	-0.7244 ±j13.3649
-0.0344 ±j7.0239	-0.0351 ±j 7.0235	-0.2143 ± j7.0235
-1.0000	-0.6743 ± j0.9524	-0.6743 ± j0.9524
-0.3857	-18.2000	-18.2000
-0.0194	-1.4623	-1.4623
	-0.1296	-0.1296
	-40.0000	-0.512
	-29.3720	-40.0000
		-29.3720

Table 2 System eigenvalues at P_0=1.5 p.u., V_t=1 p.u. (X_C/X_L=0.55)

Open-loop system (Without SMES)	Closed-loop system with SMES (equal-α mode)	Closed-loop system with SMES (unequal-α mode)
-0.0987 ±j23.3368	-0.1403 ±j23.1210	-0.1403±j23.1210
-0.1411 ±j15.4550	-0.1776 ±j14.4391	-1.1777 ±j14.4391
-0.0916 ±j12.7995	-0.0550 ±j10.9784	-0.2509 ±j13.3739
-0.0554 ±j10.9782	-0.0545 ±j10.9776	-0.4157 ±j10.9764
0.2551 ±j10.9773	**0.1554 ±j10.9776**	**-0.2525 ±j10.9764**
-0.0545 ±j10.9780	-0.0349 ± j7.0235	-0.1850 ±j10.9807
-0.0347 ± j7.0232	-0.0355 ± j7.0229	-0.1967 ± j7.0236
-0.0353 ± j7.0232	-0.0346 ± j7.0227	-0.1336 ± j7.0242
-0.0350 ± j7.0226	-0.0249 ± j5.0288	-0.1857 ± j7.0212
-0.0250 ± j5.0289	-0.0542 ± j0.4970	-0.4021 ± j5.0282
0.0717 ± j1.7393	-0.0541 ± j0.4970	-0.1981 ± j0.5735
-1.0000	-19.2108 ±j58.1324	-19.2108 ±j58.1326
	-18.2000	-18.2000
	1.3286	-0.3100
	-40.0000	-0.4310
		-40.0000

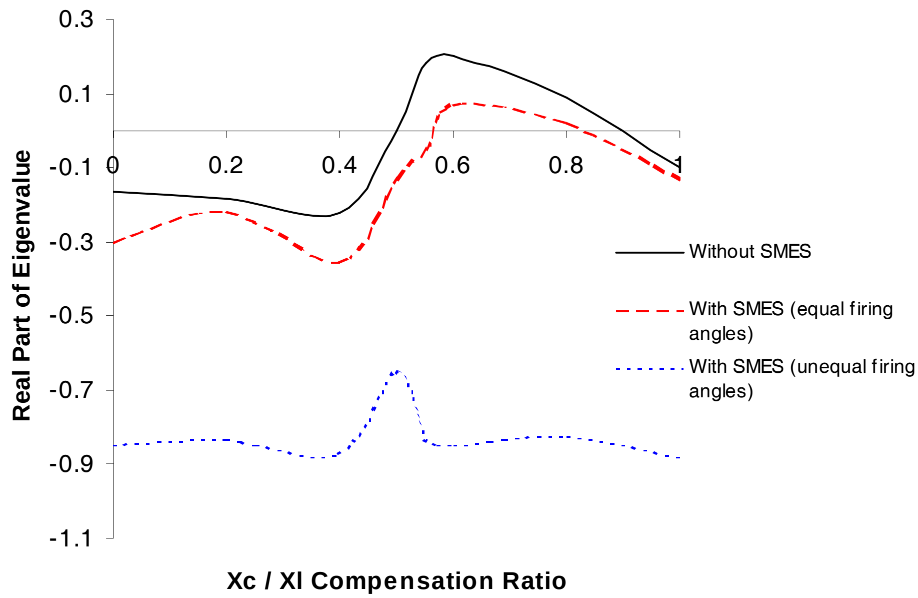

Fig. 7 Real part of electromechanical mode eigenvalue under different values of series compensation

In order to observe and survey the robustness of the proposed controller under various load conditions, the real part of the eigenvalues of the electromechanical mode versus active power outputs of generator (P_0) is plotted in Fig. 8 for three control schemes that are without SMES, with the SMES under equal α-mode and with a SMES under unequal α-mode. The capacitor is omitted from the AC transmission line in this study. The system is stable up to P_0= 1.05 p.u., without the SMES unit. The stability margin of the system with SMES under equal-α mode of operation is increased to 1.2 p.u. While the stability margin of the system with SMES under unequal- mode of operation is above P_0= 1.6 p.u. The system stability margin is greatly enlarged by the SMES under unequal-α mode of operation.

8. DYNAMIC SIMULATIONS

To further examine the damping effect of the proposed controller of the SMES unit, time-domain approach based on a nonlinear system model under disturbance conditions is performed in this section. All the nonlinearities such as the exciter ceiling voltage limit and the current limit of the super-conducting inductor have been taken into account. The system under study has been simulated using EMTDC/PSCAD program [26].

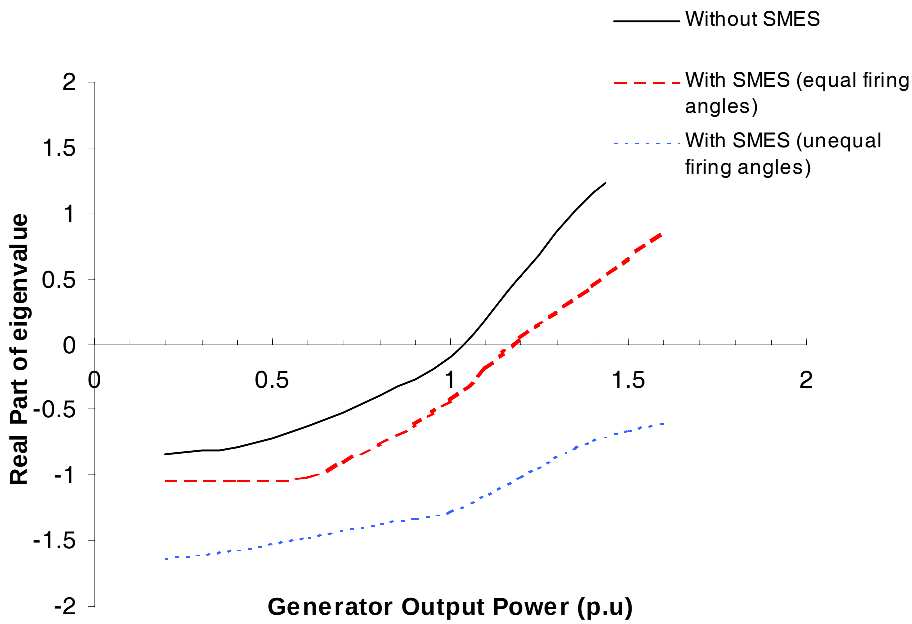

Fig. 8 Real part of electromechanical mode eigenvalue under different load conditions

It is assumed that the turbine-generator is operating at steady state delivering rated power to the infinite-bus system. To verify this condition the multi-mass system has been enabled at 0.1 sec. The plot time step is 0.05s for all the figures given in this section. The dynamic performance is examined for a large disturbance. A five-cycle three-phase short circuit fault is simulated at the transmission line near the infinite bus bar (point P of Fig. 2). The fault is applied at t=1sec and is assumed to last for 5 cycles, i.e. 0.083 s (on a 60Hz basis). Attention has been given to the dynamic response of the generator shaft, i.e. the electromagnetic torque (Te), the torque between high pressure and low-pressure turbines (T_{hl}) and the torque between low-pressure turbine and generator (T_{lg}). Time domain waveforms due to a three-phase short fault without and with the use of the SMES controller have been compared. Figs. 9 and 10 show the dynamic responses of the system without and with the use of the SMES unit respectively when P_o=1 p.u. The generator active power P_g and reactive power Q_g during the fault are given in the fourth and fifth plots of Fig. 9 respectively. The active and reactive power modulation given by the SMES unit P_{SM} and Q_{SM} are given respectively in the fourth and fifth plot of Fig. 10. The results show that, without using the SMES unit, there is almost no damping at P_o=1 as shown in Fig. 9, The shaft systems of turbine-generators are subjected to high torsional forces, which may lead to severe disturbances in the mechanical shaft.

When the SMES unit under unequal-α mode of operation is used, the damping of the synchronous generator can be greatly enhanced and the stability margin can be extended as shown in Fig. 10. It can also shown that, using an SMES unit will reduce the high torsional forces on the turbine-generator shafts to almost normal steady state values and the settling time decreases substantially.

The proposed control algorithm does not require any additional / supplementary control loops as proposed in other studies which are using equal α-mode to obtain satisfactory damping.

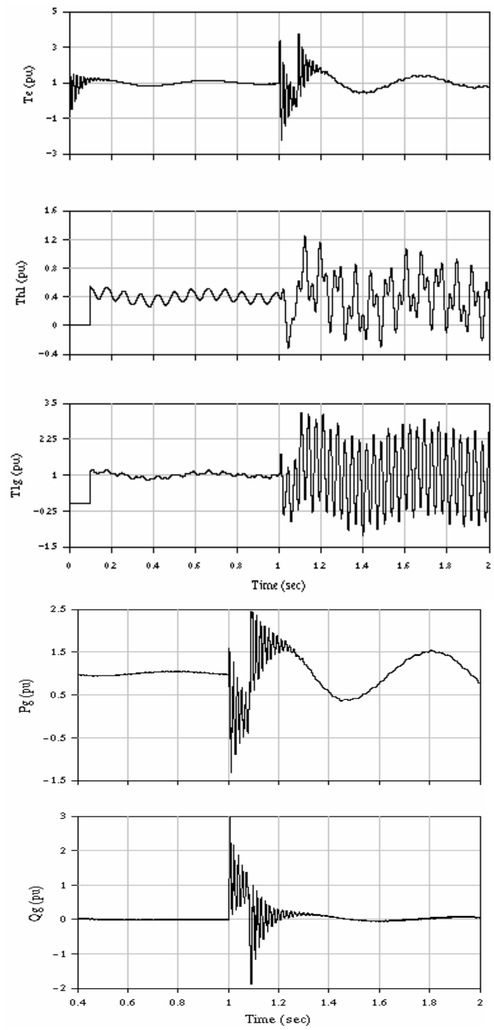

Fig. 9 System performance under large disturbance P_0= 1pu (without SMES)

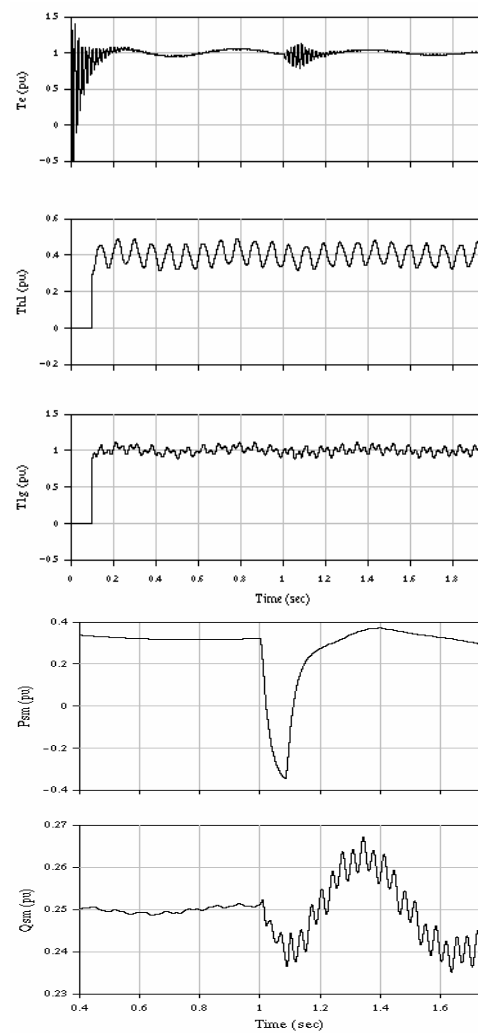

Fig. 10 System performance under large disturbance P_0=1pu (with SMES)

9. CONCLUSIONS

In this paper, an active and reactive power simultaneous modulation SMES unit is proposed to enhance torsional mode damping of the turbine-generator. The SMES control loop gains are determined using the Frequency-domain approach based on eigenvalue analysis. Two control algorithms are discussed; they are equal-α mode and unequal-α mode of operation. The frequency-domain and time-domain methods have been employed to validate the effectiveness of the proposed SMES controller. Results show the following specified conclusions:

- SMES under equal-α mode of operation is not effective in suppressing SSR and there is no improvement in the power system unless an extra controller is added.
- The additional degree of freedom provided by the SMES under unequal-α mode of operation, significantly improves the system performance.

- Eigenvalue analysis shows that, the proposed unequal-α control can render all SSR modes insensitive to different operating conditions.
- Dynamic responses without and with the proposed SMES controller of the system subject to a severe 5-cycles three-phase short-circuit fault have clearly shown that the effectiveness of the proposed SMES controller on damping unstable common-mode torsional oscillations.
- The proposed controller is very simple and does not require additional controller for the correction of desired firing angles. This controller would require very little hardware to implement.

10. ACKNOWLEDGEMENTS

The authors would like to gratefully express their thanks to the Department of Electrical and Computer Engineering, Curtin University of Technology, Australia, for providing facilities to conduct this work and for providing a Scholarship to the first author to pursue his Ph. D.

11. REFERENCES

[1] Yu, Y. N. 1983. *Electric Power System Dynamics*.

[2] Hold, M. C. and Hodges, D. A. 1976. *Experience with 500 kV subsynchronous resonance*. CH1066-0-PWR, New York: IEEE Publication, 76 p.

[3] Rabbani, M. G.; Devotta, J. B. X.; and Elangovan, S. 1999. Application of simultaneous active and reactive power modulation of SMES Unit under unequal alpha-mode for power system stabilization. *IEEE Transactions on Power Systems* 14: 547-552.

[4] Wang, L. 1991. Damping of Torsional Oscillations Using Excitation Control of Synchronous Generator: The IEEE Second Benchmark Model. *IEEE Trans. on Energy Conversion* 6: 47-54.

[5] Wang, L. and Hsu, Y. 1988. Damping of Subsynchronous Resonance Using Excitation Controllers and Static Var Compensators. *IEEE Trans. on Energy Conversion* 3: 6-13.

[6] Hamouda, R. M.; Iravani, M. R.; and Hackam, R. 1989. Damping Subsynchronous Oscillations in Power Systems Using a Static Phase-Shifter. *IEEE Trans.* PWRS-4: 889-896.

[7] Iravani, M. R. and Mathurf, R. M. 1986. Damping Supsynchronous Oscillations in Power System Using a Static Phase-Shifter. *IEEE Trans.* PWRS-1: 76-83.

[8] Hingorani, N. G.; Bhargava, B.; and Garrigue, G. F. 1987. Prototype NGH Subsynchronous Resonance Damping Scheme: Part-1-Field Installation and Operation Experience. *IEEE Trans.* PWR-2: 1034-1039.

[9] Larsen, E. V. and Swann, D. A. 1981. Applying power system stabilizers. *IEEE Trans. power Appar. and Syst.* PAS-100: 3017-3046.

[10] Hosseini, S. H. and Mirshekar, O. 2001. Optimal control of SVC for subsynchronous resonance stability in typical power system. In *Proceedings of IEEE International Symposium on Industrial Electronics, ISIE 2001.*

[11] Ukai, H.; Matsubara, H.; Kobayashi, M.; and Kandoh, H. 1997. Stabilizing control of series capacitor compensated power system on the basis of reduced order model. In *Fourth International Conference on Advances in Power System Control, Operation and Management, APSCOM-97*.

[12] Eitelberg, E.; Balda, J. C.; Boje, E. S.; and Harly, R.G. 1988. Stabilizing SSR Oscillations with A Shunt Reactor Controller. *IEEE Trans.*

[13] Boenig, H. J. and Hauer, J. F. 1985. Commissioning Test of the Bonneville Power Administration 30 MJ Superconducting Magnetic Energy Storage Unit. *IEEE Transactions on Power Apparatus and Systems* 2: 302-312.

[14] Rogers, J. D.; Barron, M. H.; Boenig, H. J.; Dean, J. W.; Schermer, R. I.; and Criscuolo, A. L. 1983. Superconducting Magnetic Energy Storage for a BPA Line Stabilization. *IEEE Transactions on Magnetics* 19: 1078-1080.

[15] Bonwick, W. J. 1997. Application of Superconducting Magnetic Energy Storage for Fluctuating Load Compensation. Energy Research and Development Corporation, Canberra.

[16] Tripathy, S. C.; Kalantar, M.; and Balasubramanian, R. 1991. Dynamic and Stability of Wind and Diesel Turbine Generators with Superconducting Magnetic Energy Storage Unit on an Isolated Power System. *IEEE Trans. on Energy Conversion* 6: 579-585.

[17] Banerjee, S.; Chatterjee, J. K.; and Tripathy, S. C. 1990. Application of Magnetic Energy Storage Unit as Load Frequency Stabilizer. *IEEE Trans.* EC-5: 46-51.

[18] Abu-Siada, A. W.; Keerthipala, W. L.; and Lawrance, W. B. 2002. Application of a Superconducting Magnetic Energy Storage unit to improve the Stability Performance of Power Systems. In *IEEE ccece02 Proceedings; ISBN: 0-7803-7514-9*. 1: 212-217.

[19] Abu-Siada, A.; Islam, S.; and Lawrance, B. 2003. Application of a Superconducting Magnetic Energy Storage unit in an HVDC system. *Presented at AUPEC'3, ISBN : 0-473-09867-9*. New Zealand, 104 p.

[20] Abu-Siada, A. and Islam, S. 2003. A novel application of Super Conducting Magnetic Energy Storage units in HVDC systems. *Presented at The 4th Postgraduate Electrical Engineering and Computer Symposium; ISBN: 0-86905-886-3*. Australia.

[21] Arsoy, A. B.; Liu, Y.; Ribeiro, P. F.; and Wang, F. 2003. STATCOM-SMES. *IEEE Industry Applications Magazine*.

[22] Mohan, N.; Undeland, T. M.; and Robbinsi, W. P. 1995. *Power Electronics Converters, Applications, and Design*. 2nd edition: John Willey & Sons.

[23] Kassakian, J. G.; Schlect, M. F.; and Verghese, G. C. 1991. *Principles of Power Electronics*: Addison-Wesley.

[24] Rabbani, M. G.; Devotta, J. B. X.; and Elangovan, S. 1999. Application of simultaneous active and reactive power modulation of SMES Unit under unequal α–mode for power system stabilization. *IEEE Trans. on Power System* 14: 547-552.

[25] Wu, C. J. and Lee, Y. S. 1993. Application of simultaneous active and reactive power modulation of SMES Unit to damp Turbine-Generator Subsynchronous Oscillations. *IEEE Trans. on Energy Conversion* 8: 63-70.

[26] Manitoba HVDC Research Centre. 1994. PSCAD/EMTDC: Electromagnetic transients program including dc systems.